Bioelectrochemistry 75 (2009) 117–123

Contents lists available at ScienceDirect

Bioelectrochemistry

journal homepage: www.elsevier.com/locate/bioelechem

Electrochemical detection of glyphosate herbicide using horseradish peroxidase immobilized on sulfonated polymer matrix

Everlyne A. Songa, Omotayo A. Arotiba, Joseph H.O. Owino, Nazeem Jahed, Priscilla G.L. Baker, Emmanuel I. Iwuoha *

SensorLab, Department of Chemistry, University of the Western Cape, Private Bag X 17, Bellville, 7535, South Africa

ARTICLE INFO

Article history:
Received 14 April 2008
Received in revised form 9 January 2009
Accepted 25 February 2009
Available online 9 March 2009

Keywords:
Poly(2,5-dimethoxyaniline)
Poly(4-styrenesulfonic acid)
Horseradish peroxidase
Biosensor
Glyphosate
Herbicide
Inhibition

ABSTRACT

This paper describes the use of horseradish peroxidase (HRP) based biosensor for novel detection of glyphosate herbicide. The biosensor was prepared by electrochemically depositing poly(2,5-dimethoxyaniline) (PDMA) doped with poly(4-styrenesulfonic acid) (PSS) onto the surface of a gold electrode followed by electrostatic attachment of the enzyme HRP onto the PDMA-PSS composite film. Fourier transform infrared (FTIR) and UV–Vis spectrometry inferred that HRP was not denatured during its immobilization on PDMA-PSS composite film. The biosensing principle was based on the determination of the cathodic responses of the immobilized HRP to H_2O_2, before and after incubation in glyphosate standard solutions. Glyphosate inhibited the activity of HRP causing a decrease in its response to H_2O_2. The determination of glyphosate was achieved in the range of 0.25–14.0 μg L^{-1} with a detection limit of 1.70 μg L^{-1}. The apparent Michaelis–Menten constant (calculated for the HRP/PDMA-PSS biosensor in the presence and absence of glyphosate was found to be 7.73 μM and 7.95 μM respectively.

1. Introduction

Glyphosate [N-(phosphonomethyl)glycine] is an important herbicide, and is a broad-spectrum, nonselective herbicide for control of long grasses and broad-leaved weeds. It interferes with the formation of amino acids and other chemicals in plants [1,2]. Glyphosate has three groups (amine, carboxylate and phosphonate) that should coordinate strongly to metal ions, particularly to transition metals [3,4]. It has been reported to possess a high affinity and chelating capacity for iron (Fe) and other metals, resulting in the formation of poorly soluble glyphosate-metal complexes or insoluble precipitates in soil or hard water [5]. As glyphosate is of comparatively low acute and chronic toxicity to human and animal health, it has become the most extensively used herbicide worldwide. Its residues can be found in soil, atmosphere, agricultural products, as well as in ground water. However, because its effects on non-target organisms and overall environmental impact have not been fully investigated, questions regarding the environmental safety with its increasing use have to be addressed. A simple analytical method for the determination of glyphosate at the sub μg L^{-1} level has proved to be very difficult to obtain, mainly due to its ionic character, low volatility, high solubility in water, insolubility in organic solvents, low mass and favored complexing behavior [6]. Most methods developed until now require pre- or post-column derivatization procedures to improve both the chromatographic behavior and the detection ability by gas chromatography (GC) or high-performance liquid chromatography (HPLC) [7,8]. For these reasons there is an expanding need for analytical method able to provide rapid, sensitive, easy and reliable detection of glyphosate at low concentrations and costs.

Biosensors appear well suited to complement standard analytical methods for the detection and quantification of glyphosate. Biosensors are defined as analytical devices incorporating a biological recognition element (enzyme, antibody, whole-cell, DNA, receptor or microorganisms) which is integrated within a physicochemical signal transducer or transducing micro system. The signal transducing element (electrode, optical detector, piezo crystal etc.) converts the biochemical response into electric and optic signals which are amplified, measured and decoded by an appropriate electronic unit [9–16]. Among the most well documented biosensors are the enzymatic ones that use enzymes as the biological recognition element. Enzyme biosensors based on inhibition of cholinesterase activity are the most commonly used. With these biosensors, the target analyte selectively inhibits the activity of the immobilized enzyme resulting in a decrease in signal that is proportional to the amount of target analyte present in test solution.

Horseradish peroxidase (HRP) in particular has served a unique role in the understanding of enzyme reactions in general and in the development of spectroscopic approaches to elucidate molecular or electronic structural properties and relevant functions [17,18]. It is a member of the large class of heme peroxidases which catalyze the oxidation of organic and inorganic substrates by H_2O_2 or organic peroxides. Most heme peroxidases contain iron (III) protoporphyrin IX

* Corresponding author. Tel.: +27 21 959 3054; fax: +27 21 959 1562.
E-mail address: eiwuoha@uwc.ac.za (E.I. Iwuoha).

1567-5394/$ – see front matter © 2009 Elsevier B.V. All rights reserved.
doi:10.1016/j.bioelechem.2009.02.007

(ferriprotoporphyrin IX) as the prosthetic group. The iron is capable of undergoing oxidation and reduction (usually to +2 and +3). HRP is the most commonly used enzyme for practical analytical applications, mainly because it retains its activity over a broad range of pH and temperature [19]. From analytical point of view, one interesting feature of HRP immobilized electrode is its low operating potential (close to 0 V versus Ag/AgCl) which offers low background currents and minimizes the risk of surface fouling and interference by electroactive species [20]. Facilitation of the electron transfer between HRP and the bare electrode surface has been very challenging. Thus, numerous efforts have been devoted to improving the electrochemical reaction of HRP by modifying the electrode surface using surfactant matrix, membranes, nanoparticles, hydrogel polymers, microcapsule or conducting polymers [21,22]. Incorporation of HRP onto conducting polymer film leads, in principle, to the enhancement of charge transport and its physical (and often chemical) stability [23]. Studies have shown that further incorporation of polyelectrolytes or dopants during polymerization maintains the conductivity of the polymer film at neutral pH [24].

This paper describes a simple and reliable procedure for preparing HRP based biosensor for the novel detection of glyphosate. Firstly, the PDMA-PSS composite film was prepared by electrochemical deposition onto the gold electrode surface. PSS was used as a dopant to maintain the conductivity of PDMA at pH 6.10. The prepared PDMA-PSS film was used as a substrate for electrostatic attachment of the heme protein HRP and it also served as an electron transfer redox mediator shuttling electrons between the immobilized HRP and the gold electrode surface. The resulting biosensor (HRP/PDMA-PSS/Au electrode) was then applied for the detection of glyphosate. The substrate H_2O_2 was used to study the activity of the biosensor before and after its contact with glyphosate standard solutions.

2. Experimental

2.1. Reagents and instrumentation

Horseradish peroxidase (E.C. 1.11.1.7, 169 U/mg powder), hydrogen peroxide, disodium hydrogen phosphate, potassium dihydrogen phosphate, hydrochloric acid, sulfuric acid, 2,5-dimethoxyaniline, poly(4-styrenesulfonic acid), N,N-dimethylformamide (DMF) and glyphosate salt were all obtained from Sigma-Aldrich (South Africa). All chemicals were of analytical grade and were used as received. All solutions were prepared with doubly distilled water.

Voltammetric and amperometric measurements were performed on a BAS 100B electrochemical analyzer from Bioanalytical Systems, Inc. (West Lafayette, IN) with conventional three-electrode system consisting of gold disk (1.6 mm diameter) as the working electrode, platinum wire as the auxiliary electrode, and Ag/AgCl (saturated 3 M NaCl) as the reference electrode. Phosphate buffer solution (0.1 M PBS, pH 6.10) was used as supporting electrolyte except for the pH dependent experiments which were performed in PBS at various pH values. All experimental solutions were purged with high-purity nitrogen gas and blanketed with nitrogen atmosphere during measurements. The experiments were carried out at controlled room temperature of 22 °C. All potentials were quoted with respect to Ag/AgCl. Amperometric measurements were carried out at an applied potential of −0.28 V while stirring. After background current reached a steady value, standard H_2O_2 solutions were added into the solution, and the steady state currents produced recorded as response.

The FTIR spectra of PDMA-PSS film before and after immobilization of HRP, including the free HRP, were recorded on PerkinElmer Spectrum 100, FT-IR Spectrometer. After electrodeposition of PDMA-PSS and immobilization of HRP, the samples were scrapped from the electrode surface and their spectra recorded without mixing with KBr. UV–Vis spectra were recorded on a Nicolet Evolution 100 Spectrometer (Thermo Electron Corporation, UK). After electrodeposition of PDMA-PSS and immobilization of HRP onto the PDMA-PSS film, the samples were dissolved in DMF and their UV–Vis spectra recorded. Free HRP sample was dissolved in PBS, pH 6.10 and its spectrum recorded.

2.2. Preparation of PDMA-PSS/Au electrode

Prior to the experiment, the bare gold electrode was polished with aqueous slurries of 1.0, 0.3 and 0.05 μm alumina powder rinsing with distilled water after polishing with each grade of alumina. The polished electrode was then sonicated in water and absolute ethanol. The counter electrode was cleaned by burning in a flame for several minutes and the Ag/AgCl electrode was cleaned by rinsing with copious amounts of distilled water.

The PDMA-PSS composite film was prepared by electrochemical polymerization of 2,5-dimethoxyaniline (DMA) in 1.0 M HCl in the presence of a dopant PSS (DMA-PSS ratio of 2:1) and electrodeposition on gold electrode surface. The potential was cycled repeatedly from −0.2 to +0.8 V, at a potential scan rate of 40 mV s^{-1}. Electropolymerization was stopped after six voltammetric cycles. Electrochemical behaviour of PDMA-PSS/Au electrode was then investigated in 1.0 M HCl solution by cyclic voltammetry (CV) in the potential range between −0.2 and +0.8 V.

2.3. Preparation of HRP/PDMA-PSS/Au electrode

Following deposition of PDMA-PSS film onto the electrode surface, the electrode was transferred to a batch cell containing PBS and the polymer surface reduced at a constant potential of −0.5 V until the reduction attained steady state. 60 μl of 2.0 mg/ml buffer solution of HRP was then added to the cell containing 1.0 ml fresh PBS and the PDMA-PSS film oxidized for 20 min at +0.65 V. During the oxidation process, the heme protein HRP became electrostatically attached onto the PDMA-PSS film. The biosensor was stored in PBS at 4 °C when not in use.

2.4. Detection of glyphosate

Cyclic voltammetry was used to measure the responses of HRP to H_2O_2 before and after its interaction with glyphosate standard solutions at controlled room temperature of 22 °C. The effect of glyphosate on HRP was studied using HRP in solution as well as that immobilized on gold electrode. The biosensor was placed in PBS (pH 6.10), 0.7 μM H_2O_2 solution added and stirred then the initial response of the biosensor measured in a quiescent solution and recorded. The reduction current generated in this case is proportional to the concentration of H_2O_2 before incubation of the biosensor in glyphosate standard solution and is a measure of the activity of the immobilized enzyme. Various concentrations of glyphosate standard solutions were then added to the working PBS containing the 0.7 μM H_2O_2 while stirring, followed by incubation of the biosensor for 20 min after each addition of glyphosate. The response of the biosensor was measured again in a quiescent solution after successive incubations and recorded. The current generated (after incubation of the biosensor) as a result of the reduction of H_2O_2 is correlated to the glyphosate concentrations. Glyphosate was added in increasing concentrations in order to determine the percentage inhibition at the various concentrations. From the data obtained, the inhibition degree (percentage inhibition, I %) was calculated as follows:

$$I\% = \frac{I_0 - I_i}{I_0} \times 100 \quad (1)$$

where I_0 and I_i are the current differences obtained for the biosensor in the absence and presence of glyphosate respectively. The same procedure was used for HRP in solution except that the measurement was carried out after the interaction of the enzyme with glyphosate for 5 min. The electrode modified with PDMA-PSS was dipped into the cell containing 2.0 ml PBS, 60 μl of 2.0 mg/ml buffer solution of HRP

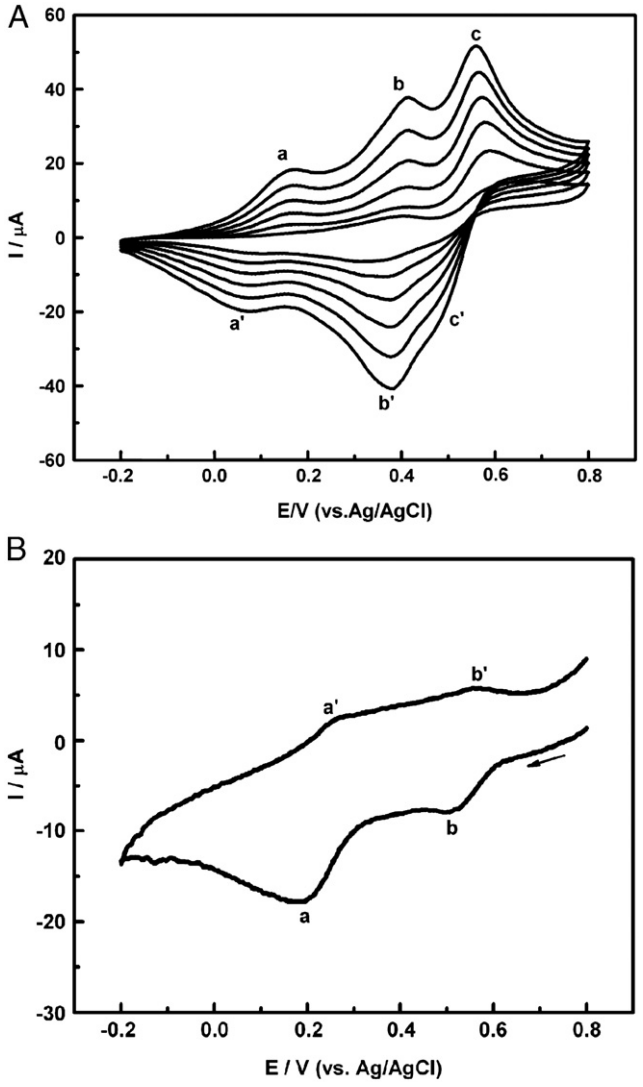

Fig. 1. Cyclic voltammograms for (A) electrochemical synthesis of PDMA-PSS, scan rate of 40 mV s^{-1} and (B) Electrochemical behaviour of PDMA-PSS/Au electrode in 1.0 M HCl.

and 0.7 μM H_2O_2, followed by additions of increasing concentrations of glyphosate and measurement of the currents generated.

3. Results and discussion

3.1. Electrochemical synthesis and behaviour of PDMA-PSS composite film

Electrochemical synthesis of PDMA-PSS resulted in deposition of a polymer film onto the surface of gold electrode. Cyclic voltammogram for electrochemical synthesis of PDMA-PSS film (Fig. 1A) showed two main redox processes (a/a′ and c/c′) corresponding to transition from leucoemeraldine to emeraldine and emeraldine to pernigraniline states. Another redox process corresponding to incorporation of oligomers into the polymer matrix or degradation products of the polymer was noticed (b/b′). The electrochemical behaviour of PDMA-PSS/Au electrode was studied in 1.0 M HCl solution by cyclic voltammetry, and the results are shown in Fig. 1B. Two pairs of redox peaks centred at +0.20 V (a/a′) and +0.56 V (b/b′) can be observed for the modified electrode (Fig. 1B). The peaks at +0.20 V correspond to the transformation of leucoemeraldine base to emeraldine salt while those at +0.56 V correspond to transformation of emeraldine salt to pernigraniline salt [25]. The absence of the redox peaks that correspond to incorporation of degradation products in Fig. 1B shows that they are less important. These results confirm that PDMA-PSS film was successfully attached onto gold electrode surface. PDMA being a polyaniline derivative shows features characteristic of polyaniline. The polyelectrolyte PSS played a major role in providing counterions for doping the synthesized PDMA to the highly conducting emeraldine salt form enabling its application at pH values between 5 and 8. The most conductive form of polyaniline is the emeraldine salt form that occurs between approximately +0.20 and +0.60 V vs. Ag/AgCl. It is known that when polyelectrolytes are incorporated as dopants into polyaniline, the switch from conducting to non-conducting material is shifted to very high pH values, enabling electrochemistry of polyaniline to be performed in neutral solutions [24].

3.2. Spectroscopic analysis of PDMA-PSS and HRP/PDMA-PSS films

Horseradish peroxidase (HRP) was the biological component of the biosensor and was immobilized electrostatically onto the PDMA-PSS/Au electrode.

The interaction between PDMA-PSS and HRP was evaluated by FTIR spectroscopy and the spectra of free HRP, PDMA-PSS and HRP/PDMA-PSS films are presented in Fig. 2. Fig. 2a shows the spectrum of electrosynthesized PDMA-PSS. The absence of the $-NH_2$ band at 3540–3200 cm^{-1} (Fig. 2a) is indicative of polymerization process. The band at 1499 cm^{-1} is due to the *para*-linked polymerization and confirms the presence of 1,4-amino (–NH–) substituted aromatic compound (1525–1485 cm^{-1}). The anionic polyelectrolyte PSS, serves a critical function of preferentially aligning the dimethoxyaniline monomers prior to polymerization promoting a more ordered *para*-linked reaction [26]. As expected, the doped form of PDMA shows the double bond character of C=N stretching frequency at 1662 cm^{-1} with PSS as the dopant. The presence of sharp duplex peaks at 1328 and 1255 cm^{-1} is characteristic of C–O groups.

The results indicated that HRP did not denature and its integral structure was not altered during its immobilization onto PDMA-PSS/Au electrode. This conclusion was verified by comparing the FTIR spectra of free HRP and HRP immobilized onto PDMA-PSS film. It is well known that the shapes and positions of the amide I and amide II infrared absorbance bands of proteins provide detailed information regarding the secondary structure of polypeptide backbone chain –CO–NH– in both naturally occurring and artificial proteins [27,28]. The amide I band (1700–1600 cm^{-1}) is caused by C=O stretching vibrations of the peptide linkages. The amide II band (1620–1500 cm^{-1}) results from a combination of N–H in plane bending and C–N stretching vibrations of the peptide groups [29]. These two amide bands are sensitive markers for protein conformation changes. Free HRP showed an IR signal at 1643 cm^{-1}

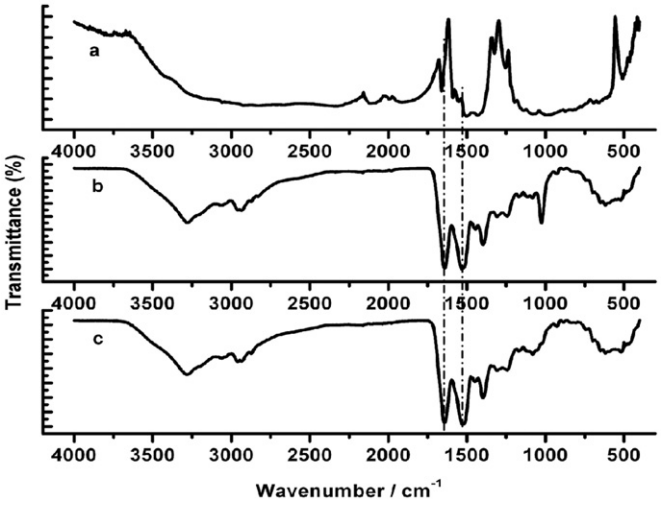

Fig. 2. FTIR spectra of (a) PDMA-PSS film, (b) HRP/PDMA-PSS film and (c) free HRP.

for amide I band, and another one at 1528 cm^{-1} for amide II band (Fig. 2c), whereas the amide I band for HRP/PDMA-PSS film appeared at 1642 cm^{-1} and the amide II band at 1530 cm^{-1} (Fig. 2b). It is observed that PDMA-PSS does not show absorbance in the amide I and amide II band regions as those of HRP and HRP/PDMA-PSS. The IR peaks at 1642 and 1530 cm^{-1} for HRP/PDMA-PSS film are thus attributed to those of amide I and II bands of HRP, occurring at similar positions as free HRP.

The position of Soret absorption band of the heme provides information regarding the tertiary structure of heme proteins; especially with regards to conformational changes in the heme region [30,31]. UV–Vis spectroscopy is therefore an effective means for monitoring the possible change of the Soret absorption band in the heme group region. Fig. 3 shows the UV–Vis spectra of PDMA-PSS, free HRP and HRP/PDMA-PSS in PBS-DMF mixture. The Soret band for free HRP appears at 409 nm (Fig. 3a) while for HRP/PDMA-PSS it is slightly shifted to 415 nm (Fig. 3b). The slight shift in Soret band for HRP/PDMA-PSS and the decrease in its absorbance may be due to the interaction between PDMA-PSS film and protein during immobilization. Such interactions do not destroy the structure of the biomolecules, thus HRP was successfully attached and retained its biological activity after immobilization on PDMA-PSS modified electrode. The spectrum of PDMA-PSS film (Fig. 3c) does not show any absorption near absorption wavelength of HRP, thus the band of HRP/PDMA-PSS at 415 nm is entirely due to HRP Soret band. The strong peak in the region around 800 nm for PDMA-PSS film is due to the polaron → π* band transition for emeraldine salt form of polyaniline. This polaron band is a diagnostic test for the conformation of the polyaniline chains and it appears in the region 750–850 nm [26].

3.3. Application of HRP/PDMA-PSS/Au electrode

3.3.1. Principle of detection

The possible electrocatalytic mechanism for HRP immobilized on the electrode surface can be expressed as follows [32]:

$$\mathrm{HRPFe(III)} + \mathrm{H_2O_2} \rightarrow \mathrm{Compound\ I} + \mathrm{H_2O} \quad (2)$$

$$\mathrm{Compound\ I} + 2e^- + 2H^+ \rightarrow \mathrm{HRPFe(III)} + \mathrm{H_2O} \quad (3)$$

When immobilized on the electrode surface, HRP can display unique bioelectrocatalytical properties in the reduction reaction of H_2O_2, by direct electron transfer from the electron-donating electrode through the active site of the enzyme and to the peroxide in solution

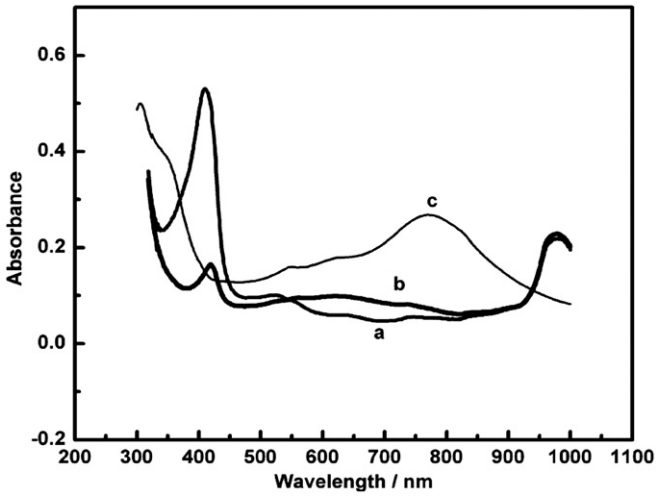

Fig. 3. UV–Vis spectra of (a) free HRP, (b) HRP/PDMA-PSS and (c) PDMA-PSS in PBS-DMF solution.

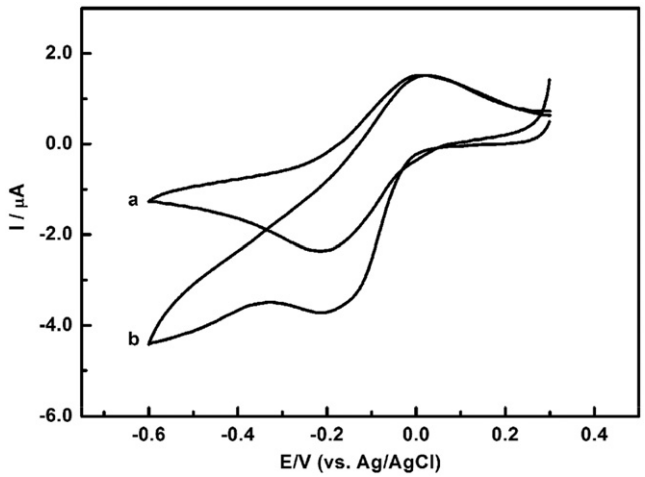

Fig. 4. Cyclic voltammograms for HRP/PDMA-PSS/Au electrode in PBS (pH 6.10) in absence of H_2O_2 (a) and in presence of 0.6 μM H_2O_2 (b), at scan rate of 5 mV s^{-1}.

[33]. However, the direct electron transfer from the bare electrode surface to the active site of the enzyme (Eq. (3)) is usually hampered by its low rate resulting from the deep burying of the electroactive groups within the protein structure due to unfavorable orientations of the molecules at the electrode surface and the long electron transfer distance between the electrode surface and the active site of HRP [33]. In the presence of a mediator such as PDMA-PSS, the heterogeneous direct electron transfer of Eq. (3) can be carried out at a reasonable rate. In this study, the electrocatalytic activity of the HRP/PDMA-PSS/Au electrode towards the reduction of H_2O_2 was investigated by cyclic voltammetry before being incubated in glyphosate. The response of the immobilized HRP to its substrate H_2O_2 is a measure of its activity. Fig. 4 shows the cyclic voltammograms for the HRP/PDMA-PSS/Au electrode in PBS (pH 6.10) in the absence and presence of H_2O_2. When 0.6 μM H_2O_2 was added into the PBS solution, the biosensor showed a remarkable increase in reduction peak current indicating that the immobilized HRP retained its bioelectrocatalytic activity and was not denatured. The steady-state responses of the biosensor to H_2O_2 were then studied in order to establish the linear range of the biosensor to H_2O_2 (data not shown). The biosensor exhibited a linear range from 0.1–0.7 μM. High electrocatalytic activity of the biosensor was certainly facilitated by good mediating capabilities of the conducting PDMA-PSS films capable of fast electron transfers.

The ability of certain compounds to inhibit the biocatalytic activity of enzymes can be exploited for their detection and quantification in the so-called enzyme-inhibition biosensor. Enzyme inhibitors are molecules that bind to enzymes thus decreasing their activity. The binding to the immobilized enzyme or the enzyme in solution results in a decrease in biosensor signal. Studies on HRP inhibition have shown that when an inhibitor is introduced into the sample solution, it can coordinate with compound I resulting in the decrease of the reduction current [34]. The reduction of the enzyme activity by inhibitors leads to a decrease in signal production that is directly proportional to the concentration of the inhibitor in the test solution. Typically, the percentage of inhibited enzyme (*I*%) that results after exposure to the inhibitor is quantitatively related to the inhibitor (i.e. analyte) concentration and the incubation time [35]. The mode of enzymatic inhibition is variable from one inhibitor to another, and may be reversible or irreversible. The response of the enzyme sensor provides a continuous measure of the activity of the immobilized enzyme, whether or not its inhibitor is present. Enzyme sensors thus allow convenient and rapid study of the inhibition of enzymes and their subsequent reactivation. In this study, the fact that herbicides suppress the activity of photosynthetic enzymes in plants has been exploited for the detection and quantification of glyphosate. The

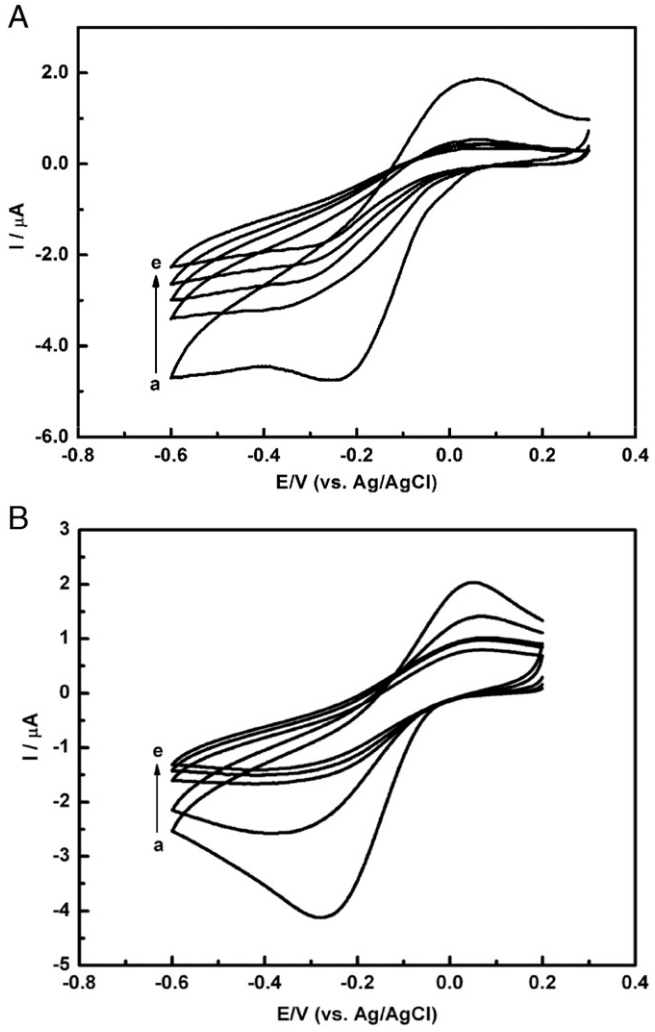

Fig. 5. Cyclic voltammograms for (A) HRP in PBS (pH 6.10) in the presence of 0.7 μM H_2O_2 after the interaction with 0.25, 6.0, 12.0, 13.0 and 14.0 μg L^{-1}glyphosate solutions (a–e) and (B) the HRP/PDMA-PSS/Au electrode in PBS (pH 6.10) in the presence of 0.7 μM H_2O_2 after incubation for 20 min in 0.25, 6.0, 12.0, 13.0 and 14.0 μg L^{-1}glyphosate solutions (a–e). Scan rate of 5 mV s^{-1}.

detection principle was based on the inhibition of the activity of HRP by glyphosate.

3.3.2. Detection of glyphosate

To study the inhibition effect of glyphosate on HRP, experiments were first performed with the enzyme in solution then with HRP immobilized on PDMA-PSS modified electrode. The initial response of HRP to H_2O_2, corresponding to its initial activity was measured followed by the measurement of its response after incubation in glyphosate phosphate buffer solution. Incubation is the stage at which the biosensor is kept in contact with the inhibitor. It allows inhibition in spite of the low rate of complexation between the enzyme and the inhibitor. The incubation time used for the experiments was obtained by measuring the response of HRP to H_2O_2 after incubation in 3.0 μg L^{-1} standard glyphosate buffer solutions for a period of 5 to 30 min (data not shown). The percentage inhibition corresponding to incubation time was then calculated using Eq. (1). For immobilized HRP, it was observed that the degree of inhibition increased with increase in incubation time and this favored the detection of glyphosate at low concentrations. In order to investigate the kinetics of inhibition and to obtain lower detection limits for the biosensor, incubation time that gives a percentage inhibition greater than 10% is preferable. Thus, the incubation time of 20 min was selected for the biosensor measurements.

The cyclic voltammograms for HRP in solution and immobilized HRP in response to H_2O_2 after contact with subsequent concentrations of glyphosate standard solutions are illustrated in Fig. 5A and B respectively. The responses were measured after incubation of the enzyme in 0.25–14.0 μg L^{-1} glyphosate standard solutions in the presence of 0.7 μM H_2O_2. Decrease in reduction peak currents with increase in glyphosate concentrations were observed in both cases demonstrating that glyphosate inhibited the activity of the enzyme HRP both in solution and when immobilized on the electrode surface. When the enzyme was in solution, inhibition occurred within 5 min and therefore longer incubation time was not necessary. At a fixed concentration of the substrate, the current measured only depends on the activity of the enzyme. Thus, the determination of glyphosate was realized according to the inhibition degree of glyphosate to HRP. Having proven that glyphosate exhibited the same inhibitory effect on HRP whether in solution or immobilized on the electrode surface, the application of the biosensor for the detection of glyphosate was to our major interest. The fact that one biosensor could be used to perform five measurements presented in Fig. 5B suggests that glyphosate is a reversible inhibitor. The experiments also showed that after contact with glyphosate, the activity of the enzyme could be recovered by simply rinsing with PBS. There was excellent sensor-to-sensor reproducibility as characterized by the low relative standard deviation of 5.0% in response of three HRP sensors (prepared at different times) to 6.0 μg L^{-1} glyphosate.

In order to obtain the glyphosate concentration that caused 50% inhibition (IC_{50}) after incubation of the biosensor for 20 min, the percentage inhibition (*I*%), derived from the results in Fig. 5B, were calculated (using Eq. (1)) and plotted against glyphosate concentrations as shown in Fig. 6. The IC_{50} value obtained from the plot was ca. 10.0 μg L^{-1}. It was observed that the percentage inhibition increased with increase in concentration of glyphosate and about 68 ± 2.5% of the activity of the immobilized HRP was inhibited by 14.0 μg L^{-1} glyphosate. The percentage inhibition calculated for HRP in solution also increased with increase in concentration of glyphosate though the inhibition was to a smaller extent compared to those achieved for immobilized HRP after incubation for 20 min. This indicates that shorter incubation time can be used for the detection of glyphosate though at lower concentrations of glyphosate, it would not be possible to attain the IC_{50} value required for the study of the type and kinetics of inhibition. The detection limit for glyphosate by this biosensor was found to be 1.70 μg L^{-1} (0.01 μM) based on the 10% inhibition degree [34,35].

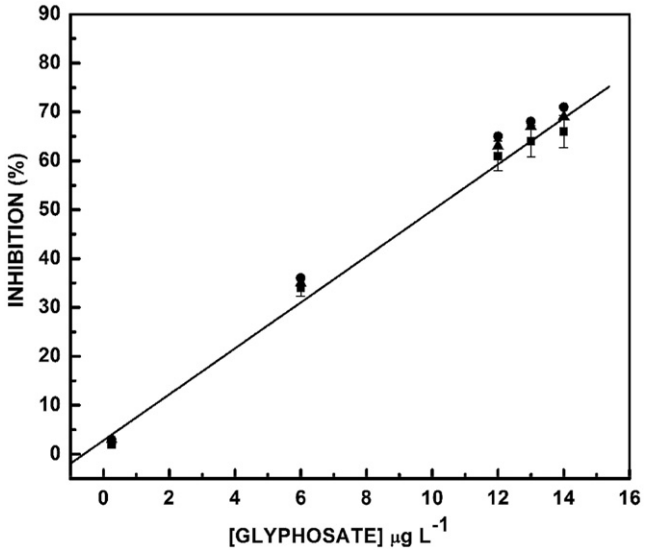

Fig. 6. Inhibition plot for the HRP/PDMA-PSS/Au electrode. Data are given as mean ± S.D. for three experiments.

To study the type and kinetics of inhibition, the response of the biosensor to various concentrations of H_2O_2 was investigated by steady-state amperometry (at applied potential of −0.28 V) in PBS (pH 6.10) in absence and presence of 10.0 μg L^{-1} glyphosate (IC_{50} value) as shown in Fig. 7A and the data obtained used to plot a Lineweaver–Burk plot for the enzymatic reaction as shown in Fig. 7B. The typical current-time response curves for the HRP/PDMA-PSS biosensor in Fig. 7A show rapid rise in reduction currents when aliquots of H_2O_2 are added into the buffer solution until steady-state values are achieved. In the presence of glyphosate, lower current values were recorded. The apparent Michaelis–Menten constant (is a reflection of both the enzyme affinity and the ratio of microscopic kinetic constants. It can be observed from the electrochemical version of the Lineweaver–Burk equation [36]:

$$\frac{1}{I_{ss}} = \frac{1}{I_{max}} + \frac{K_m^{app}}{I_{max}[S]} \quad (4)$$

where I_{ss} is the steady-state current after addition of H_2O_2, I_{max} is the maximum current measured under saturated substrate conditions and [S] is the substrate concentration in the bulk solution. From Fig. 7B, the value of the biosensor was found to be 7.73 μM and 7.95 μM

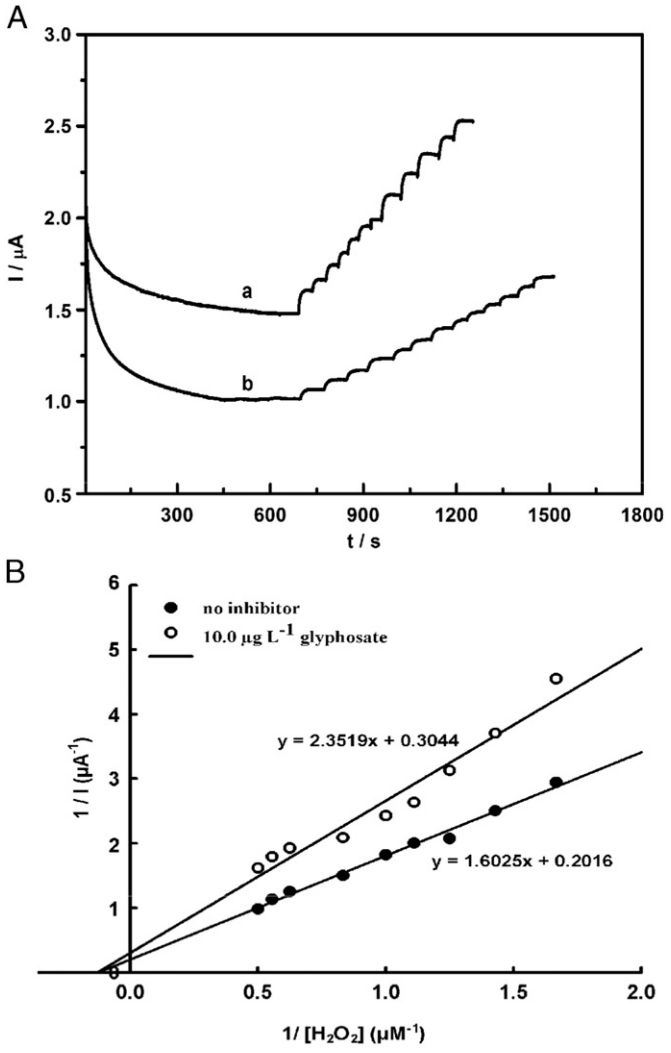

Fig. 7. (A) Amperometric responses of HRP/PDMA-PSS/Au electrode to successive injections of 0.2–2.0 μM H_2O_2 in stirring PBS (applied potential of −0.28 V) in the absence of glyphosate (a) and in the presence of 10.0 μg L^{-1} glyphosate (b). (B) Lineweaver–Burk plot for the biosensor response to H_2O_2 in absence and presence of 10.0 μg L^{-1} glyphosate.

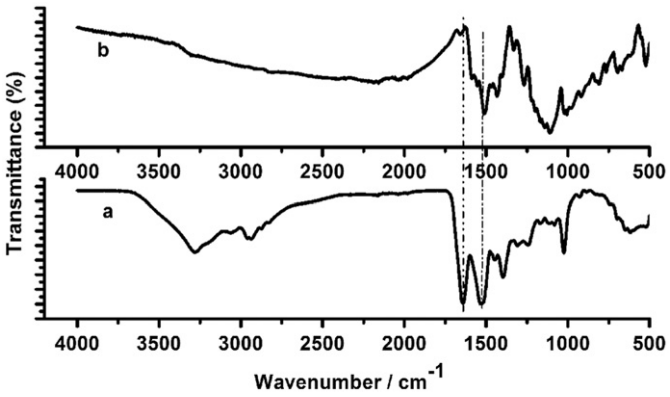

Fig. 8. FTIR spectra of (a) HRP/PDMA-PSS and (b) HRP/PDMA-PSS after its interaction with glyphosate standard solutions.

in the presence and absence of glyphosate respectively. The value was determined by analyzing the slope and intercept for the plot of the reciprocals of the cathodic current versus H_2O_2 concentration. The low values obtained for the HRP/PDMA-PSS biosensor indicates that it exhibits a high affinity for H_2O_2. Since the values obtained in presence and absence of glyphosate are in close agreement with each other, it is concluded that was unchanged during inhibition. The I_{max} values were calculated to be 4.96 μA and 3.29 μA in absence and presence of glyphosate respectively. This shows that the inhibition by glyphosate decreases I_{max}. It was however observed that the *x*-intercept remained the same with or without glyphosate. The general observations indicate that the inhibition of HRP by glyphosate is a reversible non-competitive type. It has been reported that non-competitive inhibition does not change K_m (i.e., it does not affect the substrate binding), decreases V_{max} (i.e., the inhibitor binding hampers catalysis) while the *x*-intercept remains the same with or without the inhibitor [35]. The possible inhibitory mechanism for glyphosate can thus be deduced as:

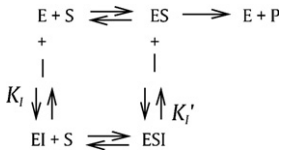

where E represents the enzyme HRP, S represents the substrate H_2O_2, I represents glyphosate and P is the product which in this case is H_2O. Non-competitive inhibitors have identical affinities for E and ES. ES represents compound I, containing an oxyferryl centre with the iron in the ferryl state (Fe^{IV}=O), and a porphyrin π cation radical.

The interaction between HRP and glyphosate was investigated by FTIR and the results are presented in Fig. 8. The changes occurring on the polypeptide backbone chain of HRP were monitored by recording the spectra of immobilized HRP before and after incubation in glyphosate. The HRP/PDMA-PSS film showed an IR signal at ca. 1642 cm^{-1} for amide I band, and another one at ca. 1530 cm^{-1} for amide II band. It was observed that the FTIR spectra recorded after the contact of the immobilized HRP with glyphosate showed the disappearance of amide I band of HRP. This clearly indicates the binding of glyphosate to HRP. Since the amide I band is attributed to C=O stretching vibration of peptide linkage in the HRP backbone, the binding by glyphosate suggests that it coordinated with the oxygen atoms in the C=O groups of HRP through its $^{+}NH_2$ group, forming a complex of HRP-Glyphosate. The formation of this complex is therefore responsible for the conformational changes of HRP. It has been reported that the changes in the microstructure of HRP obstruct the electron transfer of Fe (III) in the porphyrin cycle of the heme group, thus HRP catalytic activity is inhibited [37]. Glyphosate being a non-competitive inhibitor, it is

expected to bind to both HRP and compound I. This indicates that glyphosate inhibited the activity of HRP by obstructing the electron transfer of Fe (III) in the porphyrin cycle of the heme group therefore inhibiting its electrocatalytic activity for the reduction of H_2O_2 at the PDMA-PSS electrode surface.

4. Conclusions

HRP/PDMA-PSS/Au electrode has been successfully developed and evaluated for the novel detection of glyphosate at very low concentrations. PDMA-PSS film proves to be an attractive material for immobilization of HRP, promoting its direct electron transfer on gold electrode. The FTIR and UV–Vis results indicated that the protein HRP immobilized on PDMA-PSS film retained its bioelectrocatalytic activity towards reduction of H_2O_2 and was not denatured. Inhibition studies indicated that glyphosate inhibited the electrocatalytic activity of HRP by obstructing the electron transfer of Fe (III) in the porphyrin cycle. The electrochemical detection of glyphosate was therefore made possible by its ability to bind to HRP. The limit of detection of 1.70 μg L^{-1} achieved by this method provides therefore, sufficient sensitivity required for the determination of glyphosate in real samples. Our research is currently directed towards improvement of the performance of the biosensor as well as its evaluation for the detection of glyphosate in real samples.

Acknowledgements

Financial support from Third World Organization for Women in Science (TWOWS), Italy and National Research Foundation (NRF), South Africa is gratefully acknowledged.

References

[1] H. Kataoka, S. Ryu, N. Sakiyama, M. Makita, Simple and rapid determination of the herbicides glyphosate and glufosinate in river water, soil and carrot samples by gas chromatography with flame photometric detection, J. Chromatogr. A 726 (1996) 253–258.
[2] M.G. Cikalo, D.M. Goodall, W. Mathews, Analysis of glyphosate using capillary electrophoresis with indirect detection, J. Chromatogr. A 745 (1996) 189–200.
[3] P.G. Daniele, C. Stefano, E. Prenesti, S. Sammartano, Copper(II) complexes of N-(phosphonomethyl)glycine in aqueous solution: a thermodynamic and spectrophotometric study, Talanta 45 (1997) 425–431.
[4] E. Morillo, T. Undabeytia, C. Maqueda, L. Madrid, M. Bejarano, Cu(II)-Glyphosate system: a study by anodic stripping voltammetry and the influence on Cu adsorption by montmorillonite, Chemosphere 28 (1994) 2185–2196.
[5] B.C. Barja, J. Herszage, M. dos Santos Afonso, Iron (III)-phosphonate complexes, Polyhedron 20 (2001) 1821–1830.
[6] M.P. García de Llasera, L. Gómez-Almaraz, L.E. Vera-Avila, A. Peña-Alvarez, Matrix solid-phase dispersion extraction and determination by high-performance liquid chromatography with fluorescence detection of residues of glyphosate and aminomethylphosphonic acid in tomato fruit, J. Chromatogr. A 1093 (2005) 139–146.
[7] M. Ibáñez, O.J. Pozo, J.V. Sancho, F.V.J. Lopez, F. Hernández, Residue determination of glyphosate, glufosinate and aminomethylphosphonic acid in water and soil samples by liquid chromatography coupled to electrospray tandem mass spectrometry, J. Chromatogr. A 1081 (2005) 145–155.
[8] K. Sato, J.-Y. Jin, T. Takeuchi, T. Miwa, K. Suenami, Y. Takekoshi, S. Kanno, Integrated pulsed amperometric detection of glufosinate, bialaphos and glyphosate at gold electrodes in anion-exchange chromatography, J. Chromatogr. A 919 (2001) 313–320.
[9] B. Hock, Antibodies for immunosensors a review, Anal. Chim. Acta 347 (1997) 177–186.
[10] C.R. Suri, M. Raje, G.C. Varshney, Immunosensors for pesticide analysis: antibody production and sensor development, Crit. Rev. Biotechnol. 22 (2002) 15–32.
[11] L. Bousse, Whole cell biosensors, Sens. Actuators, B 34 (1996) 270–275.
[12] J. Wang, Electrochemical nucleic acid biosensors, Anal. Chim. Acta 469 (2002) 63–71.
[13] J. Parellada, A. Narváez, M.A. López, E. Domínguez, J.J. Fernández, V. Pavlov, I. Katakis, Amperometric immunosensors and enzyme electrodes for environmental applications, Anal. Chim. Acta 362 (1998) 47–57.
[14] M.D. Marazuela, M.C. Moreno-Bondi, Fiber-optic biosensors—an overview, Anal. Bioanal. Chem. 372 (2002) 664–682.
[15] J. Homola, S.S. Yee, G. Gauglitz, Surface plasmon resonance sensors: review, Sens. Actuators, B 54 (1999) 3–15.
[16] D.R. Thévenot, K. Toth, R.A. Durst, G.S. Wilson, Electrochemical biosensors: recommended definitions and classification, Biosens. Bioelectron. 16 (2001) 121–131.
[17] X. Chen, X. Peng, J. Kong, J. Deng, Facilitated electron transfer from an electrode to horseradish peroxidase in a biomembrane-like surfactant film, J. Electroanal. Chem. 480 (2000) 26–33.
[18] E.I. Iwuoha, I. Leister, E. Miland, M.R. Smyth, C.O. Fágáin, Reactivities of organic-phase biosensors. 1. Enhancement of the sensitivity and stability of Amperometric peroxidase biosensors using chemically modified enzymes, Anal. Chem. 69 (1997) 1674–1681.
[19] R.S. Freire, C.A. Pessoa, L.D. Mello, L.T. Kubota, Direct electron transfer: an approach for electrochemical biosensors with higher selectivity and sensitivity, J. Braz. Chem. Soc. 14 (2003) 230–243.
[20] C. Petit, K. Murakami, A. Erdem, E. Kilinc, G.O. Borondo, J.F. Liegeois, J.M. Kauffmann, Horseradish peroxidase immobilized electrode for phenothiazine analysis, Electroanalysis 10 (1998) 1–8.
[21] D. Shan, S. Wang, D. Zhu, H. Xue, Studies on direct electron transfer and biocatalytic properties of hemoglobin in polyacrylonitrile matrix, Bioelectrochemistry 71 (2007) 198–203.
[22] A.F. Collings, F. Caruso, Biosensors: recent advances, Rep. Prog. Phys. 60 (1997) 1397–1445.
[23] A. Ernst, O. Makowski, B. Kowalewska, K. Miecznikowski, P.J. Kulesza, Hybrid bioelectrocatalyst for hydrogen peroxide reduction: immobilization of enzyme within organic-inorganic film of structured Prussian blue and PEDOT, Bioelectrochemistry 71 (2007) 23–28.
[24] P.N. Bartlett, E.N.K. Wallace, The oxidation of β-nicotinamide adenine dinucleotide (NADH) at poly(aniline)-coated electrodes: Part II. Kinetics of reaction at poly (aniline)–poly(styrenesulfonate) composites, J. Electroanal. Chem. 486 (2000) 23–31.
[25] A. Morrin, O. Nagmna, A.J. Killard, S.E. Moulton, M.R. Smyth, G.G. Wallace, An Amperometric enzyme biosensor fabricated from polyaniline nanoparticles, Electroanalysis 17 (2005) 423–429.
[26] S.-C. Kim, P. Huh, J. Kumar, B. Kim, J-O. Lee, F.F. Bruno, L.A. Samuelson, Synthesis of polyaniline derivatives via biocatalysis, Green Chem. 9 (2007) 44–48.
[27] Z. Li, N. Hu, Direct electrochemistry of heme proteins in their layer-by-layer films with clay nanoparticles, J. Electroanal. Chem. 558 (2003) 155–165.
[28] Y. Liu, H. Liu, N. Hu, Core-shell nanocluster films of hemoglobin and clay nanoparticle: direct electrochemistry and electrocatalysis, Biophys. Chem. 117 (2005) 27–37.
[29] D. Sun, C. Cai, X. Li, W. Xing, T. Lu, Direct electrochemistry and bioelectrocatalysis of horseradish peroxidase immobilized on active carbon, J. Electroanal. Chem. 566 (2004) 415–421.
[30] P. George, G. Hanania, Spectrophotometric study of ionizations in methemoglobin, J. Biochem. 55 (1953) 236–243.
[31] G.-X. Ma, T.-H. Lu, Y.-Y. Xia, Direct electrochemistry and bioelectrocatalysis of hemoglobin immobilized on carbon black, Bioelectrochemistry 71 (2007) 180–185.
[32] Q. Xu, C. Mao, N.-N. Liu, J.J. Zhu, J. Sheng, Direct electrochemistry of horseradish peroxidase based on biocompatible carboxymethyl chitosan-gold nanoparticle nanocomposite, Biosens. Bioelectron. 22 (2006) 768–773.
[33] E. Ferapontova, K. Schmengle, T. Börchers, T. Ruzgas, L. Gorton, Effect of cysteine mutations on direct electron transfer of horseradish peroxidase on gold, Biosens. Bioelectron. 17 (2002) 953–963.
[34] Y. Yang, M. Yang, H. Wang, J. Jiang, G. Shen, R. Yu, An amperometric horseradish peroxidase inhibition biosensor based on a cysteamine self-assembled monolayer for the determination of sulfides, Sens. Actuators, B 102 (2004) 162–168.
[35] A. Amine, H. Mohamed, I. Bourais, G. Palleschi, Enzyme inhibition-based biosensors for food safety and environmental monitoring, Biosens. Bioelectron. 21 (2006) 1405–1423.
[36] J. Hong, A.A. Moosavi-Movahedi, H. Ghourchian, A.M. Rad, S. Rezaei-Zarchi, Direct electron transfer of horseradish peroxidase on Nafion-cystein modified gold electrode, Electrochim. Acta 52 (2007) 6261–6267.
[37] S. Guo, Q. Zhou, T. Lu, X. Ding, X. Huang, Spectroscopic studies of interactions involving horseradish peroxidase and Tb^{3+}, Spectrochim. Acta, Part A 70 (2008) 818–823.